Influence of a degraded triple-junction solar cell on the CPV system performances

C.Renno*, G.Landi, F.Petito, H.C.Neitzert
Department of Industrial Engineering, University of Salerno,
Via Giovanni Paolo II, 132, 84084 Fisciano (Salerno), Italy.

Abstract

A concentrating photovoltaic (CPV) plant is a complex system that integrates different technologies as single or multi-junction photovoltaic cells and optical devices. The CPV system performance analysis should take into account the malfunctions that can occur during the working, especially when the system operates with high values of sunlight concentration. A critical analysis of the solar cells is necessary to define the CPV system potential. In this paper a specific configuration of a CPV system is considered, and the experimental analysis of a system with a degraded triple-junction InGaP/GaAs/Ge solar cell is investigated. In particular, the triple-junction solar cell is stressed in an accelerated aging process of about 500 operating hours with a concentration of 310 suns without using a cooling system. After this process, for another 100 working hours the system has been monitored in order to compare, corresponding to different light concentration factors, the solar cell electric characteristics, the energy production and the power conversion efficiency in the pristine and degraded states. The results show the effect of the overheating of the triple-junction solar cell caused by the excessive increase of the light intensity. Under the same irradiance of 930 W/m^2 the short circuit current, open circuit voltage and fill factor values of the aged solar cell, compared to the pristine device, result to be strongly reduced, while the extracted value of the series resistance increases and the values of the shunt resistances decrease. The increased value of the diode ideality factor m after the thermal stress indicates a non-negligible contribution of non-radiative recombination within the solar cell. Similar findings are deduced comparing the electroluminescence spectra of the pristine and degraded solar cell. The thermal stress induces a marked drop of electroluminescence signal intensity in the whole investigated wavelength range. It should be note that high electroluminescence efficiency is a good indicator in solar cells for high power conversion efficiencies. In particular, the power conversion efficiency is reduced by 50% referring to a CPV system with a degraded cell, while the electric output power is decreased by 30%. Hence, it is clear that the triple-junction cell inefficiencies, principally caused by a strong thermal stress, lead to a drastic drop of the CPV system performances. Finally, an active cooling system is absolutely necessary when high values of light concentration are reached.

Key-words: CPV system, triple-junction solar cell, degraded TJ solar cell analysis, I-V characteristic.

1. Introduction

The solar technologies represent the most attractive solution in the renewable energies field because they are based on a free source available worldwide [1]. In particular, the solar energy can be adopted in different applications in order to supply primary energy [2] by means of integrated systems [3], to decrease environment pollution [4] and to meet the energy demands of different kind of users [5]. The solar technology has two crucial parameters to be optimized: the production costs and the energy conversion efficiency [6]. Due to the increasing demand for more efficient and cheaper solar systems, many researchers have focused their attention on the performance enhancement and optimization of solutions that combine different technologies such as the concentrating photovoltaic systems (CPV) [7]. These plants provide the highest solar energy conversion efficiency among all photovoltaic systems [8]. They adopt both photovoltaic and optical elements. In particular, the sunlight is focused onto the receiver, where the solar cells are placed, in order to increase the incident power per unit area. Hence, the required solar cell area for a given amount of produced electrical power decreases proportionally to the concentration factor (C) [9]. This parameter constitutes a key factor in the CPV system design and analysis. It defines how many times the incident radiation is focused onto the cell by means of the optical device. However, the increase of the incident power can also lead to a strong increase of the solar cell temperature. This could affect the conversion efficiency of the used solar cell. For this reason, in some cases, these systems adopt an active cooling mechanism in order to preserve the solar cell characteristics. This solution is represented by the concentrating photovoltaic and thermal systems (CPV/T), which allow a contemporary production of electric and thermal energy increasing the technology cost-effectiveness [10]. Among solar technologies, the triple-junction (TJ) solar cells in the last years have attracted increasing attention in the concentration solar applications because they combine a high conversion efficiency [11, 12] with a good long term stability [13]. In literature several advanced concepts such as intermediate band [14] and hot carrier solar cells [15] are investigated in order to obtain lower energy costs and higher conversion efficiencies. However, only the multi-junction solar cells, based on III-V semiconductors, have shown a power conversion efficiency over 40% [16]. To date, the best performing triple and four-junction solar cells have achieved conversion efficiencies respectively of up to 44.4 and 46% under concentrated sunlight [17]. Therefore, the use of the TJ solar cell as a receiver in the CPV system allows a drastic decrease in the balance of system costs for photovoltaic electricity generation, and makes the TJ solar cells the technology of best choice for most concentrator systems [18]. For example, a theoretical analysis and experimental verification on a CPV system, with TJ cells and an optical concentrator consisting of a Fresnel lens as primary optical element and a ball lens as secondary one, is performed in [19]. In [20] the current-voltage output characteristics of a CPV module which employs TJ solar cells is investigated under the condition of varying irradiance. Moreover, Renzi et al. have analyzed the effects of the secondary optics on the performance of a TJ solar cell used in a high concentrating photovoltaic (HCPV) system. The HCPV system is constituted by a InGaP/InGaAs/Ge TJ solar cell with a square Fresnel lens as primary optics and a refractive secondary element [21]. Previously, in [22] an experimental characterization of a CPV system, realized at the University of Salerno [9], is presented. In particular, the operation of a InGaP/GaAs/Ge solar cell is investigated under different light concentration levels. The system uses two optical devices and the monitoring of the electric energy performances, during the operating, is also provided. Hence, in order to evaluate the performances of a CPV system, the analysis of the TJ solar cell is crucial. In particular, although the TJ cell reaches the higher power conversion efficiency for a CPV system, the degradation mechanism of these devices should be understood in order to evaluate the system reliability. As reported in [23], the TJ cell malfunctions represent the main inefficiency cause in a CPV system. In particular, also if a TJ solar cell allows lower values of the charge–carrier thermalization losses, the sunlight concentration leads to an overall increase of the cell temperature when only a passive cooling is considered. This behavior can induce a wear condition due to the overheating. In literature several authors have monitored the degradation mechanisms in solar cells [24] and in optoelectronic devices under operating conditions [25]. In [26] the radiation hardness of a perovskite-based solar cell is evaluated from in situ measurements during high energy proton irradiation. As for the CPV systems, few studies report the TJ solar cell degradation used as receiver, particularly regarding the light-induced degradation tests under high irradiance levels [27]. Several experimental techniques such as electroluminescence (EL) measurements and electrical characteristics under illumination are performed in order to investigate the degradation mechanisms within the used (InGaAs/GaAs/Ge) TJ solar cell. In literature the EL analysis is extensively used to characterize the degradation phenomena for silicon [28] and organic photovoltaic devices [29]. This method is also used in order to characterize the charge carrier transport and recombination processes in the TJ solar cell

[30]. It is worth noting that the electron-hole recombination phenomena within the electronic device can be radiative or non-radiative [31]. In the first case, the loss of charge carriers occurs with the emission of a photon with an energy related to the energy bandgap of the active layer material. On the contrary for the non-radiative recombination transition, the energy associated to the carrier loss is dissipated by the crystal structure [32]. In this paper, starting from the results presented in [22], an analysis of the performances of a degraded TJ solar cell, mounted in an experimental CPV system realized previously at the University of Salerno [9], is shown. In particular, the TJ solar cell has been stressed by an accelerated aging process of about 500 hours of operating with a concentration of 310x, without any cooling mechanism. In order to monitor the TJ cell and the CPV system performances after this process, other 100 hours of operating have been monitored subsequently. This has allowed to compare the TJ cell characteristics and the CPV system energy production and efficiency values in the pristine and degraded states.

2. Experimental plant

The experimental analysis, which has allowed to investigate the degraded state of the (InGaP/GaAs/Ge) TJ solar cell, has been conducted by means of a CPV system previously realized at the University of Salerno [9]. In particular, the cell characteristics and the system electric energy output are evaluated, taking into account 500 hours of operating between 2016 and 2017. As reported in [9] the designed CPV system is based on a point focus configuration where a Fresnel lens of 32 cm constitutes the primary optics. Moreover, a secondary optics is also basic in order to uniform the incident solar radiation incident on the TJ cell and to avoid chromatic aberration problems [33]. For this purpose a kaleidoscope is adopted as shown in Figure 1, where the CPV system and the different optical solutions are reported. Hence, the secondary optics allows to improve the optical efficiency [34], while a tracking system is adopted in order to keep, in any moment, the receiver plane perpendicular to the sun rays. The Fresnel lens is set to a fixed distance of 24 cm from the kaleidoscope in the vertical direction. This focal length has allowed to reach a concentration factor of 310 suns (x) during the initial operating hours of the CPV system. As reported in Table 1, three configurations of the CPV system are used for the TJ cell analysis in the characterization and operating phases both for the pristine and degraded state. The first configuration is represented by the single TJ solar cell, on the contrary the second expects the cell and the secondary optics. In the third configuration, the Fresnel lens constitutes the primary concentrator and is added to the kaleidoscope-cell apparatus in order to obtain the complete CPV system. The system performance monitoring and the successive analysis in the degraded state are conducted following the schemes reported in Figure 2. The electric energy production of the CPV system is evaluated by means of the voltage and current measurements, which continuously have been stored with a data logger (data tracker series DT80). For this purpose, in the operating phase a variable load is connected to the TJ cell and the maximum concentration factor, that in the pristine state is of about 310x, is considered. A pyrheliometer, with an accuracy of 2%, is used for evaluating the direct normal irradiance (DNI). In order to investigate the TJ cell degradation state, its parameters are analyzed in the characterization phase. In particular, the concentration factor is varied changing the focal length of the Fresnel lens. In all the configurations, the current-voltage (I-V) characteristics are measured by using a Keithley 2400 source measurement unit (SMU, accuracy ±0.02 %). As described, one of the main causes of the TJ performances decrease is linked to the high temperature achieved during the working, where a cooling system is not provided. Hence, two thermo-resistances PT100 with an accuracy of ±0.2°C are used to monitor the cell and outdoor temperatures [35]. Finally, in order to definitively prove the wear condition of the TJ cell, an electroluminescence analysis is also conducted. The EL setup involves again the Keithley 2400 SMU. In particular, it allows to apply a constant current in order to obtain the EL measurements of the TJ solar cell. The EL spectra of the InGaP and GaAs layers are measured in the wavelength range between 200 and 1100 nm using a HR2000 High-Resolution Fiber Optic Spectrometer. On the contrary, the EL measurement system for the wavelength range between 1000 and 2000 nm, related to the Ge material light emission, consists of a mechanical chopper working at 180 Hz, a LOT-ORIEL monochromator, an InGaAs detector, a crystalline Silicon wafer as blocking filter for the lower wavelength emission and a Stanford Research “SR830” digital lock-in amplifier [36]. The use of the lock-in measurement system allows to obtain noise free measurements and therefore to detect the emission spectra at very low light intensities. The experimental measurements during the characterization phase together with the EL analysis allow to evaluate the degraded state of the TJ cell after 500 hours of operating. The uncertainty related to the evaluation of the solar cell parameters by using the fitting procedure is within 2%.

3. Analysis of the degraded state for a triple-junction cell in a CPV system

A CPV system is generally composed by three parts: the receiver, which includes the solar cell, the focusing optics and the solar tracker. In particular, under outdoor light illumination, the optics allows to concentrate, at each time, the sunlight direct component to the receiver by means of the tracking system. Hence, different problems could occur during the operating, due to the system complexity. As already reported in literature [23], the major inefficiencies of the point-focus CPV system can be related to the degradation of the photovoltaic performances of the solar cell due to the device overheating. So, the main analysis, considered in this study, investigates the difference between a TJ cell in good conditions and the same solar cell after an aging process due to 500 hours under operating condition without appropriate cooling. In particular, the InGaP/GaAs/Ge TJ solar cell in the pristine state presents a mean value of the electric power production of 2.95W and an average efficiency of 32.8% under a mean irradiance of 930 W/m^2 [22]. It should be noted that the temperature of solar cells increases considerably under light concentrating operations, whereas the conversion efficiency of the solar cells decreases when the temperature increases [37]. Hence, the temperature is one of the most specific external parameters that can accelerate the degradation rate of the solar cell performances [38]. These results have been also observed for other materials used as absorber layer in the photovoltaic system, such as polymer: fullerene [39] and perovskite [40]. In order to investigate the influence of the aging process on the CPV system, the TJ solar cell performances have been continuously evaluated for another 100 hours. The solar cell performances are compared with those observed in the pristine state, both for the characterization and for the operating phase under the same temperature condition.

3.1 The TJ cell characterization after the aging process

The TJ solar cell here investigated is formed by three p-n junctions, with InGaP, GaAs and Ge active layers respectively, stacked on top of each other and assembled with low resistive tunnel junctions, as shown in Figure 3a. These tunnel junctions are located at the interface between the sub-cells and are also optimized in order to improve the optical light coupling towards the bottom levels of the TJ solar cell. They are characterized by low electrical series resistance values [41]. At each p-n junction an ideality factor m is associated which depends on the voltage, applied to the solar cell. At high bias voltages the diffusion component becomes dominant and the ideality factor assumes a value of one. On the contrary, for the degraded device the recombination processes within the junction become significant and m approaches a value of two. The standard single diode model of a triple-junction solar cell under light illumination, is composed by one diode (D_1), a photocurrent source, a series resistor, and a shunt resistor for each sub-cell [31]. The photocurrent source is due to optical generation of the charge carriers (I_{ph}). The series resistance (R_s) depends on various components such as the electrode resistance of the metal grid, the ohmic contact between metal and semiconductor, the resistance of the semiconductor materials and the substrate layer [31]. The shunt resistance (R_{sh}) accounts for the leakage current of the solar cells [31]. As already reported, the investigated TJ device shows a dominant diffusion component in the pristine state under operating conditions with light concentration [22]. Therefore, in order to model the electrical characteristics of the TJ solar cell after the aging process, the junction recombination mechanisms are modeled adding a second diode (D_2) in parallel with the diode D_1 and setting its ideality factor to 2. The I-V characteristics of a TJ solar cell under light illumination can be modeled as the sum of three components: the diffusion current I_{diff}, the recombination current I_{rec} and the photocurrent I_{ph}. The measured I-V characteristics under light illumination can be well reproduced by:

$$I = I_{diff,i}\left\{\exp\left[\frac{e(V-IR_{s,i})}{m_{diff,i}kT}\right]-1\right\} + I_{rec,i}\left\{\exp\left[\frac{e(V-IR_{s,i})}{m_{rec,i}kT}\right]-1\right\} + \frac{V-IR_{s,i}}{R_{sh,i}} - I_{ph,i}, \qquad (1)$$

where i represents the sub-cell number (1=top, 2=medium and 3=bottom), e is the elementary charge, k is the Boltzmann constant, T is the absolute temperature, $I_{diff,i}$ and $I_{rec,i}$ are the components of the diode saturation currents related to the diffusion and recombination contributions with an ideality factors $m_{diff,i}$ and $m_{rec,i}$, respectively [42]. The used equivalent circuit of the TJ solar cell is shown in Figure 3b. The maximum output voltage corresponds to the sum of the three sub-cell voltages measured at open circuit condition (V_{oc}). On the contrary, the maximum photo-generated current results to be the lowest value of the single photo-generated currents at short circuit condition (I_{sc}). The concentration factor C is defined dividing I_{sc} under concentrated light (I_{sc} (x)) and the I_{sc} under light concentrated at one sun [43]. Hence, the concentration factor of the CPV system, experimentally evaluated, is expressed as:

$$C = \frac{I_{sc}(X)}{I_{sc}}. \qquad (2)$$

The dependence of the V_{oc} as a function of C can be expressed as

$$V_{oc} = V_{oc_{1\,sun}} + \frac{mkT}{e}\ln(C) \quad (3)$$

where $V_{oc_{1\,sun}}$ is the open-circuit voltage at one sun and m is the diode ideality factor. After the aging process, the recombination contribution within the degraded TJ solar cell becomes dominant and the effect of the diode D_1 is negligible. For the parameter estimation of the TJ solar cells, a curve fitting procedure between the measured and the theoretical I-V characteristics at different concentrations in terms of the single diode model, has been applied [38]. The power conversion efficiency (η) of the TJ solar cell under light concentration is defined as the maximum output power divided by the incident power on the cell:

$$\eta = \frac{V_{oc} \cdot I_{sc} \cdot FF}{C \cdot G \cdot A_c} \quad (4)$$

where G is the incident direct radiation and A_c the area of the solar cell. Hence, the fill factor (FF) represents the ratio between the maximum real electric power (P_c) and the product of the short circuit current and the open circuit voltage:

$$FF = \frac{P_c}{V_{OC} \cdot I_{SC}} \quad . \quad (5)$$

Therefore, the parameters V_{oc}, I_{sc}, η, m and FF represent the equivalent parameters of the TJ cell. They are evaluated referring to the aged state of the cell after about 500 hours of operating at 310x in the third configuration of the CPV system. The TJ cell analysis in the degraded state is completed by the EL measurements.

3.2 Comparison between the pristine and degraded state of the TJ cell

The CPV system, designed and equipped at University of Salerno [9], after a first characterization phase [22] has operated at a concentration of 310x in the third configuration for about six months between 2016 and 2017. The CPV plant does not include an active cooling system for the TJ cell; hence, considering the monitored cell temperature of about 70°C, the cell degradation has been considered as the main cause of failure. For this reason, the InGaP/GaAs/Ge TJ cell has been again analyzed in the characterization phase. All the measurements in the degraded state have been realized during another 100 hours after the first phase of operation. The analysis takes into account all the solar cell parameters in the pristine and degraded states. In order to investigate the role played by the sunlight concentration for the aging process, the focal length of the Fresnel lens has been changed. Under these operating conditions, C has been modified exploiting the different system configurations. In particular, the cell parameters have been analyzed using as a reference the first configuration, where the concentration ratio C is equal to 1. Subsequently, for the other two configurations the C values have to be evaluated again starting from the Equation 2. The aging process, indeed, affects the cell short-circuit current and this results in a change of the C values of the different configurations. Therefore, the C values in the second and third configuration can be expressed as:

$$C_{2\,(3)} = \frac{I_{sc,kal\,(CPV)}}{I_{sc}} \qquad (6)$$

where $I_{sc,kal}$ and $I_{sc,CPV}$ are the short-circuit current, respectively, in the second and in the third configuration. Hence, considering the same level of direct radiation, the first comparison between the pristine and the degraded states of the TJ cell considers C. Once evaluated the maximum value of C in the third configuration, corresponding to the TJ cell in wear conditions, C has been modified in order to characterize the solar cell as function of C after the aging process. This procedure has allowed to make a direct evaluation of the TJ solar cell parameters for both the operation conditions. Therefore, each parameter is a function of C and s, where s indicates the TJ state (pristine, degraded):

$$V_{oc}, I_{sc}, FF, \eta, R_s, R_{sh} = f\,(C,s) \qquad (7)$$

The TJ cell performances have been also compared in terms of electroluminescence efficiency and in the different phases of operation. In this case the EL measurements allow to investigate the difference between the emission peak wavelength and amplitude for the pristine and degraded solar cell in the electroluminescence spectra. Finally, in order to evaluate the reduction of the performances of the CPV system in terms of the real electric power (P) and power conversion efficiency, the system performance during a new operating phase with the degraded TJ cell, used as a receiver of the CPV system, has been monitored. It is worth noting that the percentage reduction of the electric output in the degraded state represents a key evaluation point for the CPV system.

4. Results and discussion

The performances monitoring of the CPV system, used to evaluate some problems in the electric energy output, consists of the measurement for about 100 hours of operating condition under light soaking. The CPV system performance drastically decreased from the initial phase of operating. This behavior has been immediately correlated to the TJ cell degradation. In particular, the main observed problem has been the cell overheating due to the lack of an active cooling system [44]. In Figure 4, the energy production in the third configuration has been reported, corresponding to the initial C value of 310x. In particular, considering eight hours a day and the same irradiance conditions of 890 W/m^2, the tests compare the electric energy output in the first hours of operating with data obtained in the days following the 500 hours of operation. The estimated produced electrical energy, in the first phase, reached a value of about 23.5 Wh for a single TJ cell. The tests in an advanced state of aging for the TJ cell have showed an average reduction of about 45.8%, considering the same outdoor conditions as in the case of the first measurement. Starting from these observations, the TJ cell has been characterized in the degraded state, in all configurations and with variable C value.

4.1 Results of the degraded TJ solar cell characterization

In Table 2 all the I_{sc}, V_{oc} and C values, for the three configurations before and after the light soaking, have been reported. The effect of the overheating of the TJ solar cell caused by the light illumination performed under operating condition for 500 hours at 310x can be clearly observed in the Table 2. After the light exposure of the TJ solar cell, the measured device undergoes a strong thermal stress caused by the light concentration that accelerates the aging process. This mechanism affects the charge carrier recombination and transport processes, the performances of the TJ solar cell and, therefore, of the overall CPV system. Under a moderate light concentration factor of less than 10 suns, the I_{SC} values for the pristine and the degraded states are similar, as can be observed for the C_1 and C_2 configurations of the CPV system. On the contrary, as shown in Table 2, regarding the Voc values, a clear difference is evident. In particular, the degraded solar cell, measured at one sun and under about 7.4 suns, shows a lower value of the open circuit voltage as compared to those reported for the pristine TJ solar cell. This suggests that the electrical characteristics of the solar cell are affected by ohmic losses due to additional shunt current paths. It is worth noting that the difference in terms of V_{OC} between the pristine and the degraded state of the TJ solar cells decreases as a function of the light intensity. This result is in good agreement with that found in literature, where low values of the shunt resistance lead to additional power losses in the solar cell by providing an alternative current path for the photocurrent. The effect of a shunt resistance becomes dominant at low light intensities and at lower bias voltages and results to be negligible at higher photo-generated charge carrier densities. As a further evidence of the leakage current due to additional shunt current paths, in the configuration C_3 a slight decrease of V_{OC} value, before and after the thermal stress, of only 0.1 V has been reported. However, by using the configuration C_3 a higher value of the concentrator factor (310x) is reached for the CPV system using a pristine TJ solar cell. In this configuration, a marked drop of the short circuit current value of about 0.35A, measured for the TJ solar cell after the thermal stress, has been also observed. This reduction leads to a decrease of C of about 24% reaching a new value of 235 suns. It should be noted that the combined decrease of the V_{OC} and I_{SC} values means that by increasing the light intensity a further loss mechanism, due to the overheating, occurs in the device. In order to correlate the performance degradation of the TJ solar cell to the overall CPV system, an accurate analysis of the electrical characteristics of the CPV system adopting as a receiver, the degraded TJ solar cell as a function of the light intensity, has been done. In Figure 5a a comparison between the I-V characteristics of the aged InGaP/GaAs/Ge TJ solar cell, measured under the same direct irradiance of 930 W/m^2 using the different optic configurations of the CPV system, has been reported. As can be observed, only at a higher light concentration factor (configuration C_3) a clear change of the slope in the IV curve from 1.40 to 2.91 has been observed. This effect is clearly visible in Figure 5b where a comparison of the I-V characteristics of the TJ solar cell in the pristine and in the aged states respectively at 310 and 235 suns, is shown. Under the same irradiance, the I_{SC}, V_{OC} and the FF values of the aged solar cell as compared to the pristine device result to be strongly reduced. By considering the Equations 3-5 and the fitting method proposed by [42], the solar cell parameters V_{OC}, I_{SC}, FF, η, R_s and R_{sh} have been estimated as function of C for the aged TJ solar cell. In particular, in the Figures 6 and 7 the dependence of the TJ solar cell parameters on C has been reported. As already reported in literature, in a triple junction solar cell under concentration, an increase of the temperature leads to a monotonic decrease of the power conversion efficiency and of the open circuit voltage values [45]. In the present study, the measurements performed in the pristine and in the degraded states of the solar cell have been conducted by changing the light concentration at a fixed temperature. As indicated in Figure 6a, the V_{OC} values increase logarithmically with increasing light concentration. Considering the Equation 3, the values of the diode ideality factor m for the pristine and the aged solar cells have been extracted. In particular, after a thermal stress performed under operating condition, an increase of the m value from 2.91 to 4.45 has been observed for the TJ solar cell. A value of $m \approx 3$ for the pristine TJ cell usually indicates high quality p–n junctions and the dominance of radiative recombination. On the other hand, higher m values indicate non-negligible contributions of non-radiative recombination in at least one of the junctions [46]. This means that, after the light soaking at higher concentration, an increase of the charge carrier recombination without the emission of light occurs in the solar cell. This result, related to the overheating of the TJ solar cell under operating condition, has been already reported in literature [47]. It should be noted that besides the junctions of the top, middle and bottom cells, within the TJ there are other two tunnel junctions that can also contribute to the ohmic losses.

In Figure 6b, a monotonic increase of the I_{sc} values with increasing light intensities for both the investigated solar cells, has been observed. On the other hand, the FF of the aged solar cell remains constant at a value of 78% up to 25 suns, and then drastically decreases reaching a value of 42% at 235 suns. Compared to the values extracted for the pristine solar cells (open symbols in Figure 6c), a strong decrease of the FF has been reported. As indicated in the Figure 6d, the initial value of η has been determined to be 32% and 25% at one sun for the pristine and aged TJ solar cell, respectively. By increasing the light concentration, for both the CPV systems the efficiency increases reaching a maximum value of 39.9% at 81 suns and 30.6% at 25 suns corresponding to the FF maximum value. A further increase of the concentration causes a decrease of the efficiency for both the devices. Hence, the η value decreases down to 17.6% at 235 suns for the degraded TJ solar cell. It is worth noting that the peak value shift towards a lower light concentration of the η and FF values, observed for the degraded TJ solar cell, is due to an increase of the series resistance. In Figure 7 the series and the shunt resistance values of the pristine and degraded TJ solar cell under operating condition of the CPV system as a function of C, are shown. After the thermal stress, R_s shows values higher than that extracted for the pristine state of the TJ solar cell in the whole investigated C range. As can be observed in Figure 7a, the series resistance of the degraded device shows a value of 2.6 Ω at one sun and slight decrease with the increase of C reaching a value of 1.5 Ω at 235 suns. On the contrary, for the pristine device the R_S value at one sun is 2.2 Ω and subsequently decreases as a function of the light intensity assuming a value of 0.25 Ω at 310 suns. This result suggests that after the aging process a formation of an additional parasitic resistance R_S', estimated at 1.25 Ω at 235 suns, in series connection to the device occurs within the TJ solar cell. This additional ohmic contribution causes an increase of the series resistance values and, therefore, a marked reduction of the FF and η values which becomes important for high currents [37-40]. Additionally, the extracted value of the R_{sh} results to be lower than that calculated for the device in the pristine state being constant at about 1 KΩ at one sun, and then decreases down to a value of 132 Ω at 235 suns. For the degraded device, the ratio between the shunt and the series resistances $r= R_{sh}/R_S$ is about 400 at one sun, and becomes lower than 100 at 235 suns. As a comparison with the values calculated for the pristine TJ device as a function of C, r results to be higher than one order of magnitude compared to the aged device. This difference, reached under light concentration, suggests that the physical phenomena behind the decrease of the V_{OC} and η values are mostly due to defects within the device and along the device perimeter [48]. It is worth noting that this effect influences also the dark current value of the degraded TJ solar cell with an increase of the recombination contribution I_{rec} compared to the pristine device. As already shown in Figure 6c and 6d for the FF and the η values, a marked change of the R_s and of the R_{sh} values occurs after a threshold value of the concentration light intensity of about 25 suns. This result confirms that the degradation process takes place within the pristine TJ device under operating condition at high light intensity.

Hence, R_s slightly decreases reaching a value of 1.5 Ω whereas the R_{sh} assumes a value of 132 Ω at 235 suns, respectively. On the contrary, for the aged TJ solar cell the increase of the ideality factor m suggests that further charge carrier recombination mechanisms are present within the solar cell. It is worth noting that the electron-hole recombination phenomena within the electronic device can be radiative or non-radiative [31]. As clearly observed from the change in slopes in Figure 6a, the thermal aging leads to a change of the recombination phenomena with an increase of the non-radiative recombination pathways compared to the pristine device. In order to quantify the relation between the radiative (and non-radiative) losses and the CPV system efficiency related to the solar cell performances, the electroluminescence analysis has been performed.

4.2 EL analysis of the degraded TJ solar cell

In Figure 8a the comparison of the normalized electroluminescence spectra of the InGaP/GaAs/Ge triple-junction solar cell before and after the aging process is shown. The electroluminescence signals have been measured in the wavelength range between 500 and 2000 nm by biasing the device at a constant forward current. The measured electroluminescence emission spectra of the TJ solar cell is composed of three emission peaks located at 884 and 660 nm for the InGaP and GaAs materials (biased at 20 mA), and a broad emission peak located at about 1700 nm due to the germanium layer (biased at 50mA). Since the EL-emission peak amplitude related to the germanium bottom sub-cell results to be much lower and much more noisy in comparison with the top and the middle sub-cells, a more sensitive EL measurement setup has been used. In the Figure 8b the solid line represents the electroluminescence signal measured from the pristine TJ solar cell biased with a bias current of 50 mA. It is worth noting that the intensity of the electroluminescence peaks related to the direct Ge band-to-band transition at 1550 nm, and to the indirect Ge band-to-band transition at 1880 nm, are of the same order of magnitude [47]. The combination of these EL emission peaks in the germanium produces a broad emission signal located at about 1700 nm [22]. The spectral responsivity decrease of the InGaAs detector results in a strong reduction of the detector photocurrent for wavelengths above 1700 nm. After the de-convolution procedure, performed in order to distinguish the germanium EL-emission peak from the diffraction peaks of the monochromator grating, a broad emission peak at 1550 nm has been observed. After the thermal stress, a marked drop of the electroluminescence signal intensity in the whole investigated wavelength range has been observed. For the top and the middle-sub cells, shown in Figure 8a, a reduction of 50% and of 30% of the EL peak intensity has been reported for the InGaP and GaAs materials, respectively. Additionally, the intensity emission of the germanium bottom sub-cell is reduced by about 90%, as can be observed in Figure 8b. This result is a further indication that the aging process, performed under operating condition at 310 suns for 500 hours, produces a strong increase of the non-radiative recombination and, therefore, a decrease of the measured EL signal. It is widely reported in literature that the intensity peak of the EL spectra is proportional to the diffusion length (L_n) of the charge carriers within the junction, as a consequence, their decrease suggests a direct decrease of the L_n values [49, 50].

This is also confirmed by the increase of the diode ideality factor, estimated by the slope of the V_{OC} as a function of C, as can be observed in Figure 6a. In addition, the effect of the recombination centers has been also evidenced by the increase of the dark recombination current.

4.3 Decrease of the CPV system performances

The aged state of the TJ solar cell affects the CPV system performances in terms of electric power and power conversion efficiency. As a matter of fact, during the 500 hours of the aging process of the TJ solar cell only the real-time electric power of the CPV system has been investigated. The cooling system has been switched off and the temperature ranged between 25°C and 75°C during the day, with a constant light concentration factor of 310 suns, has been monitored. Additionally, a marked reduction of the electric power during the operation has been observed. Therefore, once characterized the TJ solar cell in order to evaluate its state of aging respect to the pristine state, different new tests have been performed with the third configuration of the designed CPV system. In particular, the Fresnel lens height has been kept at a value of 24 cm in order to compare the electrical performances respect to the previous experimental measurements. In Figure 9, the CPV electrical power has been reported for the CPV system with TJ cell respectively in the degraded and in the pristine state. As previously mentioned, with the third configuration the system has reached a value of 235x with the degraded solar cell, while the C value in the pristine state was of 310x. The tests have been done between 9:30 am and 15:30 pm; the mean electric power has been 2.05 W and 2.95 W respectively for the aged and the pristine state, with a mean irradiation value of 900 W/m^2 [51]. Hence, a reduction of about 30% can be observed for the CPV system with a TJ cell in the aged state. In Figure 10 the power conversion efficiency of the CPV system with an aged TJ cell has been analyzed in order to show its reduction with respect to the pristine conditions. In particular, a mean efficiency value of 15.8% has been obtained at 235x during the system operation. This value has been compared with the system efficiency at 310x with a TJ cell with no prior aging process. In this case, the system power conversion efficiency is decreased by about 50%. As previously reported [22], the solar cell efficiency at 700 W/m^2 has been also calculated and its mean value is nearly 26.7 %. In Table 3 the monitoring of the power conversion efficiency at different irradiation conditions for the solar cells in the pristine and aged states, has been shown. In particular, as expected the cell efficiency values in the aged state result to be always lower than in the pristine state. This result is mainly due to the high temperatures reached during the working [52]. Hence, an active cooling system [53] is basic for this type of system in order to both preserve the cell conditions and to obtain better electrical performances. Finally, the last analysis of the CPV system performance is related to the tracking system. In particular, the strategic role of the kaleidoscope as secondary optics has been highlighted. The electric energy decrease of the CPV system with a single TJ cell has been investigated in different configurations: the first with both primary and secondary optics, and the second configuration as previously described. The second is a new kind of system equipment that expects only the Fresnel lens. The analysis has been carried out considering an interruption of the tracking system during the operation for about 20 minutes. In Figure 11a, although a comparable electric energy production can be observed for the two configurations during the initial monitoring period, the system electrical energy production in the second configuration is drastically reduced in comparison with the first configuration. This is demonstrated in Figure 11b, where the energy percentage reduction of the two configuration is reported. In particular, an interruption of the tracking has resulted in a complete stop of the energy production after only 5 minutes for the configuration with only the Fresnel lens. On the contrary, the system with two optics has arrested its energy production after about 12 minutes. Hence, the secondary optics also improves the CPV system tracking process.

5. Conclusions

In this paper the influence of the degraded triple-junction solar cell on the CPV system performances has been studied analyzing the current-voltage characteristics under light concentration. As evidenced, after the accelerated aging process, induced by the overheating of the solar cell under 310 suns for 500 hours of operating conditions, a marked reduction of the power conversion efficiency value has been reported. In particular, the aged triple-junction solar cell shows an efficiency value of only about 25% at one sun, that is much lower than the 32% observed in the pristine state. For light concentration values lower than 10x, the degraded solar cell shows a lower value of the open circuit voltage as compared to the value reported for the pristine TJ solar cell. This suggests that the electrical characteristics of the device are strongly affected due to the ohmic losses in an additional shunt current path. The differences in terms of the open circuit voltage becomes negligible for increasing C and a marked drop of the short circuit current values has been observed. This means that a further loss mechanism, besides the shunt and series resistance losses, arises from the solar cell overheating which strongly influences the charge carrier recombination and transport processes within the TJ solar cell and therefore the overall CPV system. This result is consistent with that observed for the dependence of the solar cell parameters on the light concentration ratio. In particular, after the thermal aging a strong increase of the diode ideality factor value from 2.91 to 4.45 has been observed. This finding indicates that the overheating leads to the formation of additional recombination pathways due to non-radiative recombination processes. This result has been clearly noted in the electroluminescence emission spectra, where in the case of the degraded solar cell lower emission is observed. Decreases of 50% and 30% of the electroluminescence peak intensity values are reported for the InGaP and GaAs materials respectively, while for the germanium bottom sub-cell electroluminescence emission intensity is reduced by about 90%. This indicates that the non-radiative recombination mechanism results, referring to the aged device, are the dominant recombination path. As a consequence for the decreased TJ solar cell performances, the power conversion efficiency of the CPV system, which operates with the highest value of C, is strongly reduced. In particular, at 235 suns, the observed CPV system electrical efficiency with the aged solar cell results to be 15.8% lower than that measured for the pristine condition, where a value of 33.4% has been observed. Hence, the accelerated aging process observed with 500 hours of operating under high levels of light concentration induces a strong thermal stress in TJ solar cell. As a consequence it can be concluded that an active cooling system is basic to preserve the solar cell integrity and to improve the cost-effectiveness of the CPV system.

Nomenclature

A	area (m^2)
C	concentration factor
CPV	concentrating photovoltaic
CPV/T	concentrating photovoltaic and thermal
D	diode
DC	direct current
DNI	direct normal irradiance (W/m^2)
EL	electroluminescence
FF	fill factor
G	incident direct radiation ((W/m^2)
HCPV	high concentrating photovoltaic
I	current (A)
I-V	current-voltage
InGaP/GaAs/Ge	indium-gallium-phosphide/gallium-arsenide/germanium
InGaP/InGaAs/Ge	indium-gallium-phosphide/indium -gallium-arsenide/germanium
k	Boltzmann constant
m	ideality factor
P	electric power (W)
PV	photovoltaic
R	resistance (Ω)
s	state
SMU	source measurement unit
T	temperature (°C)
TJ	triple-junction
x	suns

V voltage (V)

Greek symbol

η efficiency

Subscripts

c cell

d diffusion

e electron charge

i sub-cell number

kal kaleidoscope

oc open circuit

ph photocurrent

rec recombination

s series

sh shunt

sc short-circuit

References

[1] Najibi F, Niknam T. Stochastic scheduling of renewable micro-grids considering photovoltaic source uncertainties. Energy Conversion and Management 2015; 98:484–99.

[2] Desideri U, Zepparelli F, Morettini V, Garroni E. Comparative analysis of concentrating solar power and photovoltaic technologies: technical and environmental evaluations. Applied Energy 2013; 102:765–84.

[3] Talavera, DL, Perez-Higueras PJ, Almonacid F, Fernández EF. A worldwide assessment of economic feasibility of HCPV power plants: profitability and competitiveness. Energy 2017; 119: 408–424.

[4] De Feo G, Forni M, Petito F, Renno C. Life cycle assessment and economic analysis of a low concentrating photovoltaic system. Environmental Technology 2016; 37:2473-

82.
[5] Eicker U, Demir E, Gürlich D. Strategies for cost efficient refurbishment and solar energy integration in European Case Study buildings. Energy and Buildings 2015; 102: 237–249.
[6] Tiwari B, Hossain MJ, Bhattacharya I. GaP/InGaAs/InGaSb triple-junction current matched photovoltaic cell with optimized thickness and quantum efficiency. Solar Energy 2016; 135:618–624.
[7] C. Renno and M. De Giacomo. Dynamic simulation of a CPV/T system using the finite element method, Energies, 2014; 7:7395-7414.
[8] Burhan M, Chua KJE, Ng KC. Simulation and development of a multi-leg homogeniser concentrating assembly for concentrated photovoltaic (CPV) system with electrical rating analysis. Energy Conversion and Management 2016; 116:58–71.
[9] Renno C, Petito F. Experimental and theoretical model of a concentrating photovoltaic and thermal system. Energy Conversion and Management 2016;126:516-25.
[10] Sharaf OZ, Orhan MF. Concentrated photovoltaic thermal (CPVT) solar collector systems: Part I – Fundamentals, design considerations and current technologies. Renewable and Sustainable Energy Reviews 2015; 50:1500–65.
[11] Green MA, Emery K, Hishikawa Y, Warta W, Dunlop ED. Solar cell efficiency tables (version 44). Prog Photovoltaics Res Appl 2014; 22:701–710.
[12] Green MA, Emery K, Hishikawa Y, Warta W, Dunlop ED. Solar cell efficiency tables (Version 45). Prog Photovoltaics Res Appl 2015; 23:1–9.
[13] Hong H-F, Huang T-S, Uen W-Y, Chen Y-Y. Damp-Heat Induced Performance Degradation for InGaP/GaAs/Ge Triple-Junction Solar Cell. J Nanomater 2014;2014:1-6.
[14] Marsen B, Klemz S, Landi G, Steinkopf L, Scheer R, Schorr S, et al. Phases in copper–gallium–metal–sulfide films (metal=titanium, iron, or tin). Thin Solid Films 2011; 519:7284–7.

[15] König D, Casalenuovo K, Takeda Y, Conibeer G, Guillemoles JF, Patterson R, et al. Hot carrier solar cells: Principles, materials and design. Phys E Low-Dimensional Syst Nanostructures 2010; 42:2862–6.

[16] King RR, Law DC, Edmondson KM, Fetzer CM, Kinsey GS, Yoon H, et al. 40% efficient metamorphic GaInP⁄GaInAs⁄Ge multijunction solar cells. Appl Phys Lett 2007; 90:183516.

[17] Lin T-N, Santiago SRMS, Zheng J-A, Chao Y-C, Yuan C-T, Shen J-L, et al. Enhanced Conversion Efficiency of III–V Triple-junction Solar Cells with Graphene Quantum Dots. Sci Rep 2016; 6:39163.

[18] Shanks K, Senthilarasu S, Mallick TK. Optics for concentrating photovoltaics: Trends, limits and opportunities for materials and design. Renew Sustain Energy Rev 2016; 60:394–407.

[19] Huang Q, Xu L. Ball lens as secondary optical element for CPV system. Solar Energy 2017; 148:57–62.

[20] Fernández EF, Ferrer-Rodríguez JP, Almonacid F, Pérez-Higueras P. Current-voltage dynamics of multi-junction CPV modules under different irradiance levels. Solar Energy 2017; 155: 39–50.

[21] Renzi M, Cioccolanti L, Barazza G, Egidi L, Comodi G. Design and experimental test of refractive secondary optics on the electrical performance of a 3-junction cell used in CPV systems. Applied Energy 2017; 185: 233–243

[22] Renno C, Petito F, Landi G, Neitzert HC. Experimental characterization of a concentrating photovoltaic system varying the light concentration. Energy conversion and management 2017; 138:119-130.

[23] Renno C, Miranda S, Petito F. Inefficiencies analysis of a point-focus CPV/T system. Int J Green Energy 2016; 13:918–29.

[24] Acierno D, Amendola E, Bellone S, Concilio S, Ferrara L, Iannelli P, et al. Synthesis and luminescent properties of a new class of nematic oxadiazole containing poly-ethers for PLED. J Non Cryst Solids 2004;338–340:278–82.

[25] Neitzert HC, Landi G. Temperature dependent optoelectronic properties of a non-intentionally created cleaved-coupled-cavity laser. Microelectron Reliab 2014; 54:2142–6.

[26] Lang F, Nickel NH, Bundesmann J, Seidel S, Denker A, Albrecht S, et al. Radiation Hardness and Self-Healing of Perovskite Solar Cells. Adv Mater 2016; 28:8726–31.

[27] Rey-Stolle I, Algora C. High-irradiance degradation tests on concentrator GaAs solar cells. Prog Photovoltaics Res Appl 2003; 11:249–54.

[28] Neitzert HC, Ferrara M, Kunst M, Denker A, Kertész Z, Limata B, et al. Electroluminescence efficiency degradation of crystalline silicon solar cells after irradiation with protons in the energy range between 0.8 MeV and 65 MeV. Phys Status Solidi 2008; 245:1877–83.

[29] Neitzert HC, Ferrara M, Rubino A, Concilio S, Iannelli P, Vacca P, et al. Monitoring of the initial degradation of oxadiazole based blue OLED's. J Non Cryst Solids 2006; 352:1695–9.

[30] Chen S, Zhu L, Yoshita M, Mochizuki T, Kim C, Akiyama H, et al. Thorough subcells diagnosis in a multi-junction solar cell via absolute electroluminescence-efficiency measurements. Sci Rep 2015; 5:7836.

[31] S. M. Sze and Kwok K. Ng. Physics of Semiconductor Devices. 3rd ed. Hoboken, U.S.A.: John Wiley & Sons; 2006.

[32] Landi, G., Neitzert, H.C., Barone, C., Mauro, C., Lang, F., Albrecht, S., Rech, B., Pagano S. Correlation between electronic defect states distribution and device performance of perovskite solar cells. Adv Sci 2017: 1700183.

[33] Akisawa A, Hiramatsu M, Ozaki K. Design of dome-shaped non-imaging Fresnel lenses taking chromatic aberration into account. Solar Energy 2012; 86:877–85.

[34] Chemisana D, Vossier A, Pujol L, Perona A, Dollet A. Characterization of Fresnel lens optical performances using an opal diffuse. Energy Conversion and Management 2011; 52:658–663.

[35] C.Aprea and C. Renno. Experimental model of a variable capacity compressor, International Journal of Energy Research, 2009; 33, 29-37.

[36] Landi G, Henninger M, De Girolamo del Mauro A, Borriello C, Di Luccio T, Neitzert HC. Investigation of the optical characteristics of a combination of InP/ZnS-quantum dots with MWCNTs in a PMMA matrix. Opt Mater 2013; 35:2490–5.

[37] Nishioka K, Takamoto T, Agui T, Kaneiwa M, Uraoka Y, Fuyuki T. Evaluation of temperature characteristics of high-efficiency InGaP/InGaAs/Ge triple-junction solar cells under concentration. Sol Energy Mater Sol Cells 2005; 85:429–36.

[38] Landi G, Barone C, De Sio A, Pagano S, Neitzert HC. Characterization of polymer fullerene solar cells by low-frequency noise spectroscopy. Appl Phys Lett 2013; 102:223902.

[39] Barone C, Landi G, De Sio A, Neitzert HC, Pagano S. Thermal ageing of bulk heterojunction polymer solar cells investigated by electric noise analysis. Sol Energy Mater Sol Cells 2014; 122:40–5.

[40] Barone C, Lang F, Mauro C, Landi G, Rappich J, Nickel NH, et al. Unravelling the low-temperature metastable state in perovskite solar cells by noise spectroscopy. Sci Rep 2016; 6:34675.

[41] Yamaguchi M, Takamoto T, Araki K. Super high-efficiency multi-junction and concentrator solar cells. Sol Energy Mater Sol Cells 2006; 90:3068–77.

[42] Brus V V., Lang F, Bundesmann J, Seidel S, Denker A, Rech B, et al. Defect Dynamics in Proton Irradiated $CH_3NH_3PbI_3$ Perovskite Solar Cells. Adv Electron Mater 2017:1600438.

[43] Zilong W, Hua Z, Dongsheng W, Wei Z, Zhigang Z. Characterization of the InGaP/InGaAs/Ge triple-junction solar cell with a two-stage dish-style concentration system. Energy Conversion and Management 2013; 76:177–84.

[44] C.Aprea and C. Renno. An air cooled tube-fin evaporator model for an expansion valve control law, Mathematical and Computer Modelling, 1999; 30, 135-146.

[45] Siefer G, Bett AW. Analysis of temperature coefficients for III-V multi-junction concentrator cells. Prog Photovoltaics Res Appl 2014;22:515–24.

[46] Braun A, Hirsch B, Vossier A, Katz EA, Gordon JM. Temperature dynamics of multijunction concentrator solar cells up to ultra-high irradiance. Prog Photovoltaics Res Appl 2013; 21:202–8.

[47] Korech O, Hirsch B, Katz EA, Gordon JM. High-flux characterization of ultrasmall multijunction concentrator solar cells. Appl Phys Lett 2007; 91:64101.

[48] De Kersauson M, Jakomin R, El Kurdi M, Beaudoin G, Zerounian N, Aniel F, et al. Direct and indirect band gap room temperature electroluminescence of Ge diodes. J Appl Phys 2010; 108:23105.

[49] T. Fuyuki, H. Kondo, T. Yamazaki, Y. Takahashi, and Y. Uraoka. Photographic surveying of minority carrier diffusion length in polycrystalline silicon solar cells by electroluminescence, Appl. Phys. Lett., vol. 86, no. 26, p. 262108, 2005.

[50] W. Xiao, X. He, Y. Gao, Z. Zhang, and J. Liu. Far-infrared electroluminescence characteristics of an InGaP/InGaAs/Ge triple-junction solar cell under forward DC bias, J. Semicond., 2012; 33:64008.

[51] C.Renno, F.Petito, A.Gatto. Artificial neural network models for predicting the solar radiation as input of a concentrating photovoltaic system, Energy Conversion and

Management, 2015; 106: 999-1012,.

[52] C. Renno and F. Petito. Choice model for a modular configuration of a point-focus CPV/T system, Energy and Buildings, 2015; 92, 55-66.

[53] C.Aprea and C. Renno. A numerical approach to a very fast thermal transient in an air cooling evaporator, Applied Thermal Engineering, 2002; 22, 219-228.

Tables captions

Table 1 Experimental equipment

Table 2 Comparison between the main parameters of the degraded photovoltaic cell

Table 3 Conversion efficiency at different irradiation conditions for the solar cells in the pristine and aged states

Figures captions

Figure 1 Photos of the TJ cell in different configurations

Figure 2 Scheme of the experimental measurements

Figure 3 TJ solar cell: (a) cross section; (b) DC equivalent circuit with tunnel diodes.

Figure 4 Comparison of the daily electric energy production in the pristine state and degraded states

Figure 5 (a) Comparison between the I-V characteristics measured in different conditions after the aging process; (b) I-V characteristics of the triple-junction solar cell in the pristine and degraded states at 310 and 235 suns.

Figure 6 Comparison of the solar cell parameters for the pristine and for the degraded TJ cell as function of C: (a) open-circuit voltage (V_{OC}); (b) short-circuit current (I_{SC}); (c) fill factor (FF); (d) efficiency (η).

Figure 7 Comparison of the series resistance R_S and of the shunt resistance R_{sh} as function of C for the TJ solar cell in the pristine and in the degraded states

Figure 8 Comparison between the normalized electroluminescence spectra measured for a InGaP/GaAs/Ge triple-junction solar cell biased at different injection currents: (a) I = 20 mA and (b) I = 50 mA in the pristine (dotted line) and (b) in the aged state (solid line).

Figure 9 Comparison between the measured electric powers for the TJ solar cell in the pristine and degraded states

Figure 10 Comparison between the CPV system electric efficiency values with the TJ solar cell in the pristine and degraded states

Figure 11 Tracking system problems: (a) energy losses in different configurations; (b) time for a complete interruption.

Table(s)

configuration 1	InGaP/GaAs/Ge TJ cell
configuration 2	TJ cell + kaleidoscope
configuration 3	Fresnel lens + TJ cell + Kal.
TJ cell area	5.5 x5.5 mm^2
Pristine/degraded state measurement	EL, Voc, Isc, FF, η, P

Table 1 Experimental equipment

Table(s)

Configuration	***V_{oc} (V)***		***I_{sc} (A)***		***Concentration (x)***	
	Pristine State	***Degraded state***	***Pristine State***	***Degraded state***	***Pristine State***	***Degraded state***
C1 (TJ cell)	2.56	2.27	0.00421	0.00435	1	1
C2 (kaleidoscope)	2.72	2.58	0.03117	0.0319	7.33	7.40
C3 (kal +lens)	3.01	2.91	0.98826	1.35	310	235

Table 2 Comparison between the main parameters of the degraded photovoltaic cell

	cell efficiency [%]	
Irradiance [W/m^2]	Pristine state	Aged state
900	32.8	15.8
700	26.7	14.2
500	22.5	11.3

Table 3 Conversion efficiency at different irradiation conditions for the solar cells in the pristine and aged states

Figure(s)

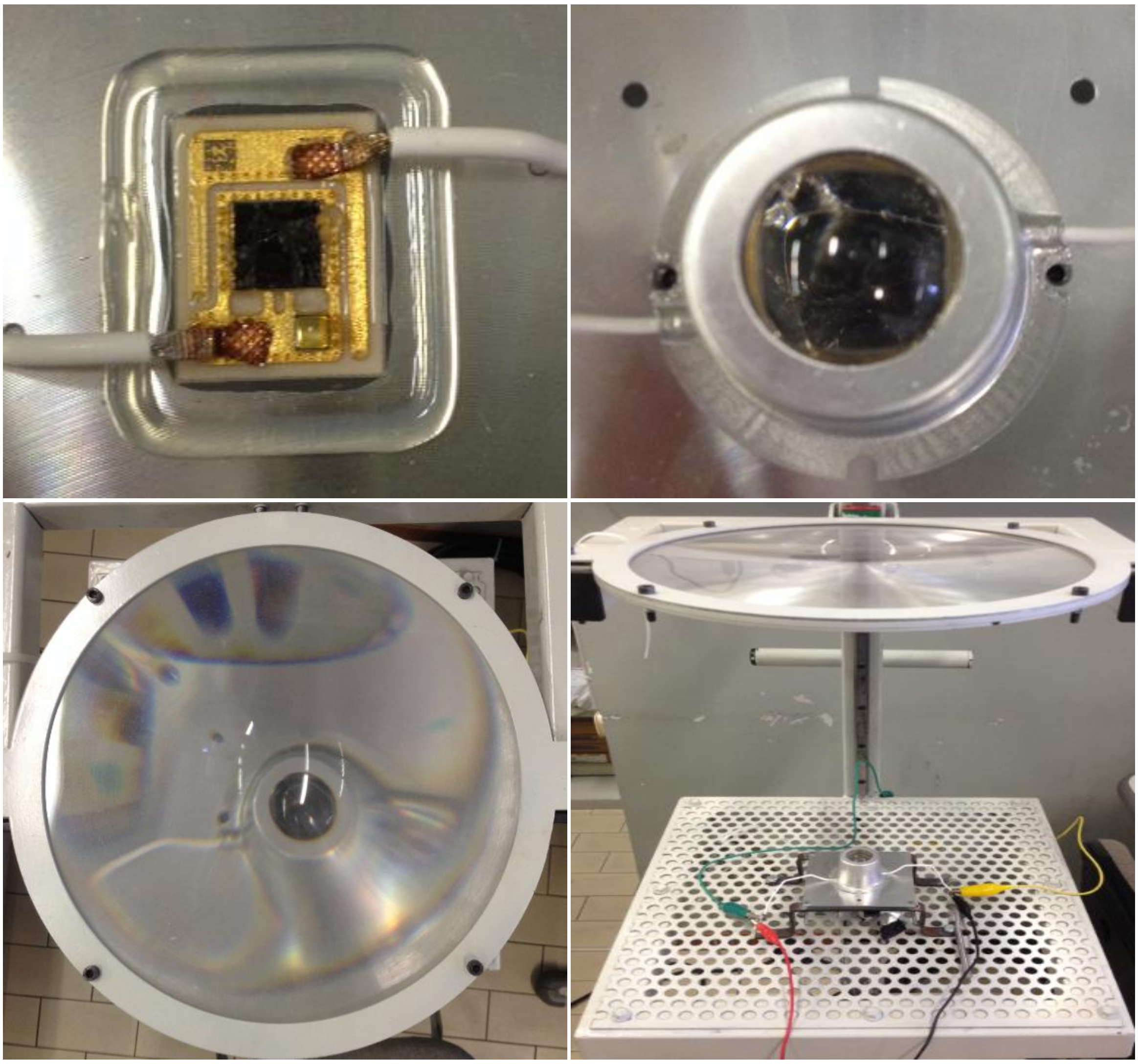

Figure 1 Photo of the TJ cell in different configurations

Figure(s)

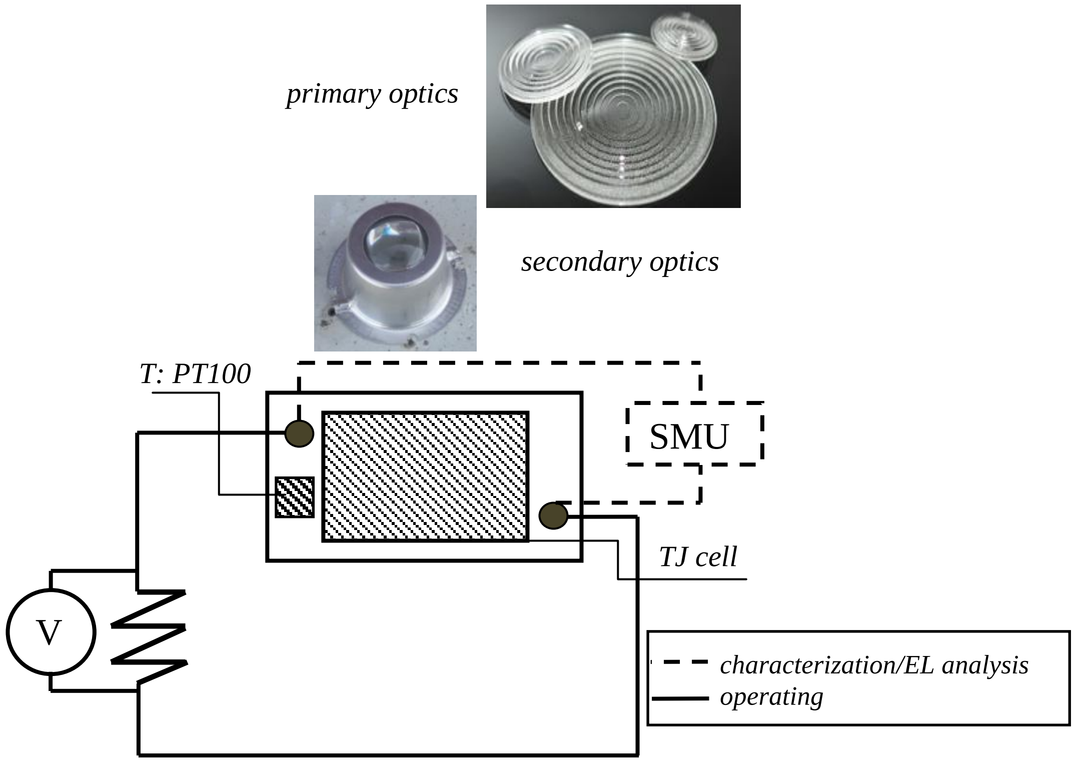

Figure 2 Scheme of the experimental measurements

Figure(s)

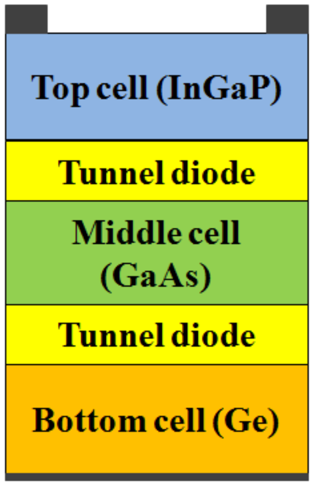

(a)

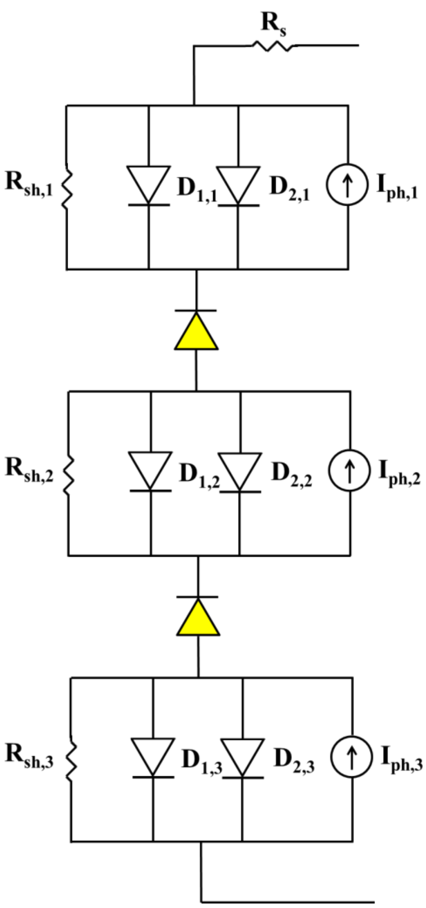

(b)

Figure 3 TJ solar cell: (a) cross section; (b) DC equivalent circuit with tunnel diodes.

Figure(s)

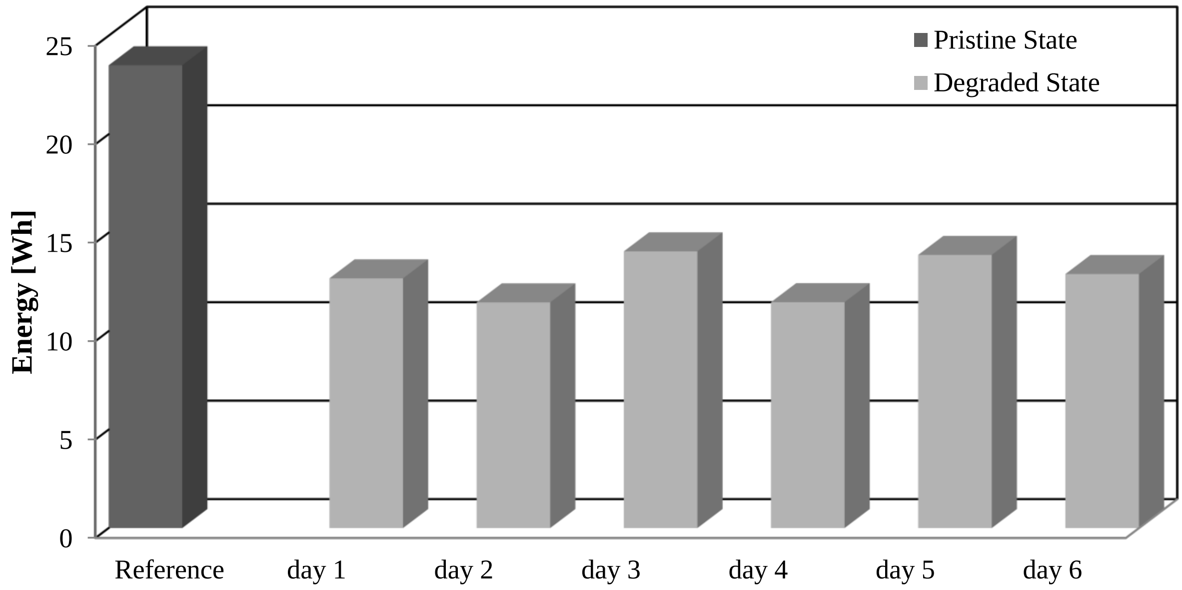

Figure 4 Comparison of the daily electric energy production in the pristine state and degraded states

Figure(s)

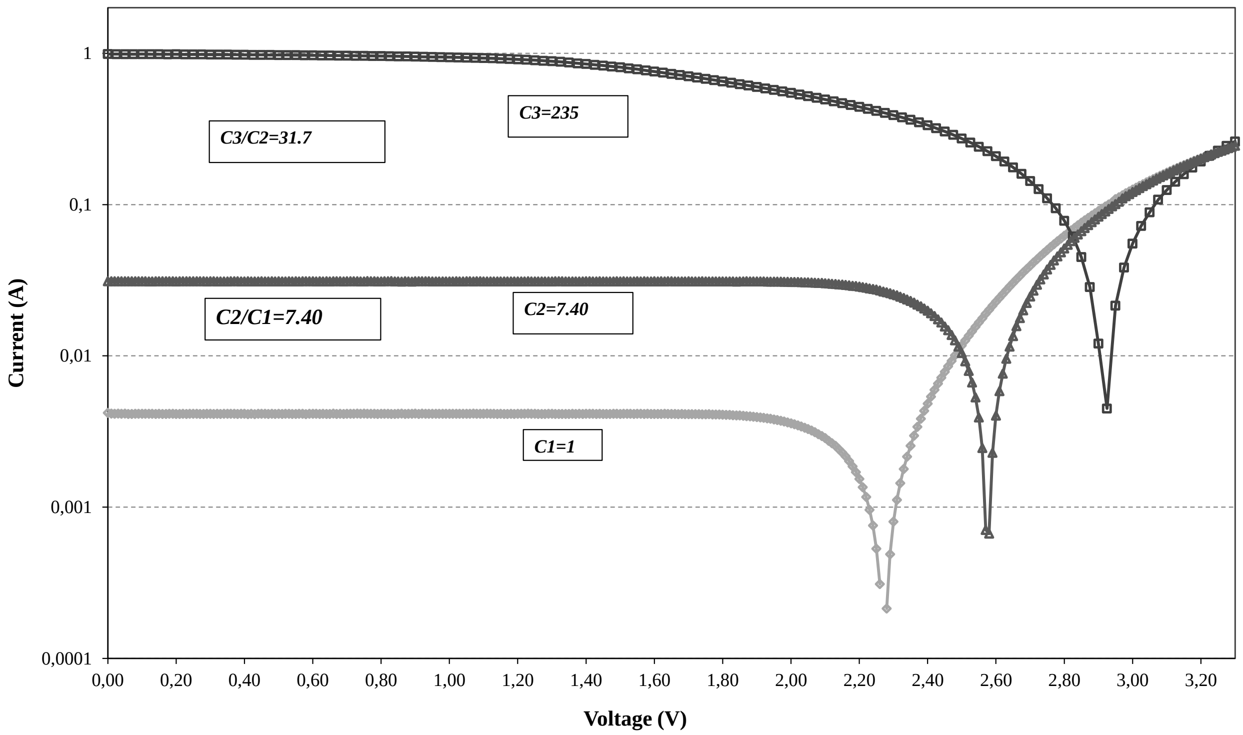

(a)

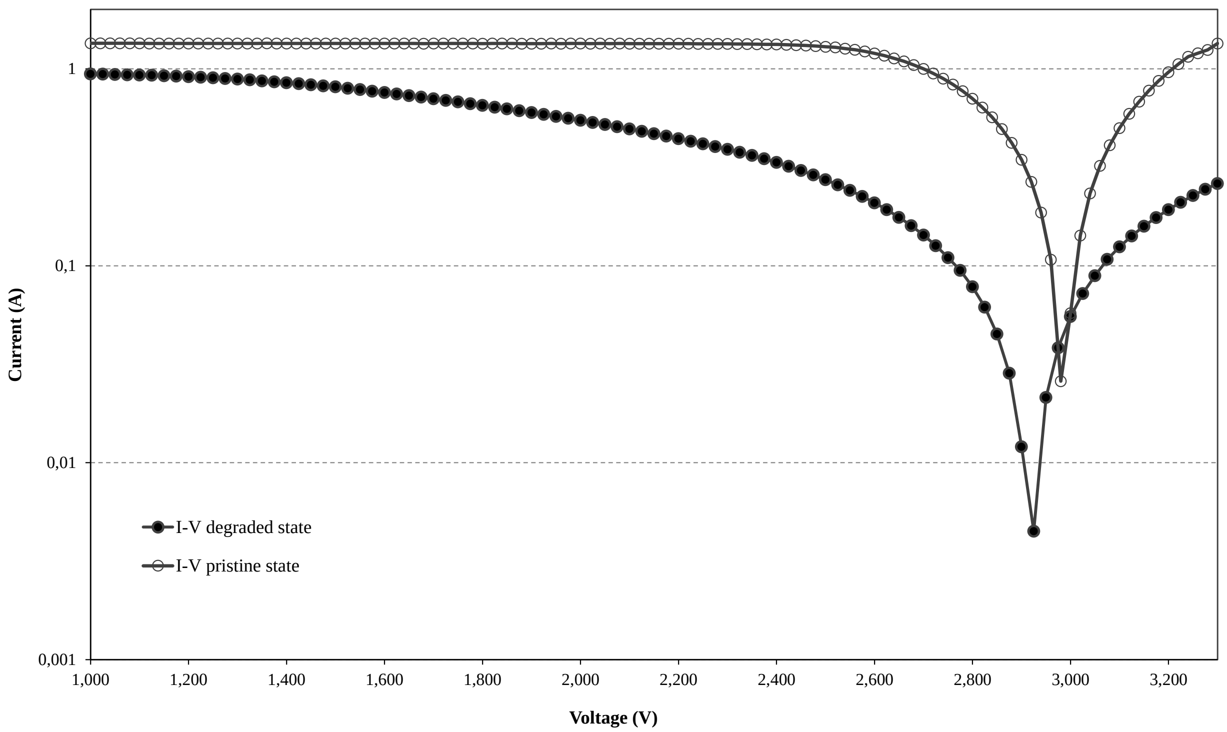

(b)

Figure 5 (a) Comparison between the I-V characteristics measured in different conditions after the aging process; (b) I-V characteristics of the triple-junction solar cell in the pristine and degraded states at 310 and 235 suns.

Figure(s)

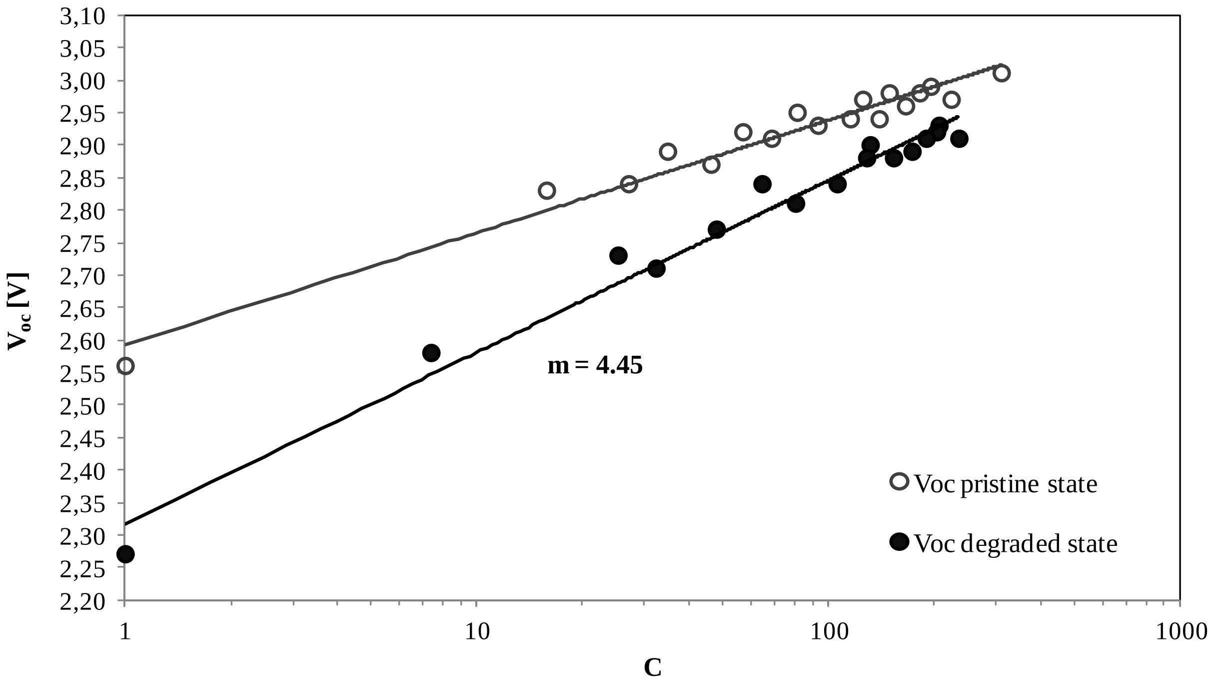

3,10
3,05
3,00
2,95
2,90
2,85
2,80
2,75
2,70
2,65
2,60
2,55
2,50
2,45
2,40
2,35
2,30
2,25
2,20
V_{oc} [V]
1
10
100
1000
C
m = 4.45
Voc pristine state
Voc degraded state

a)

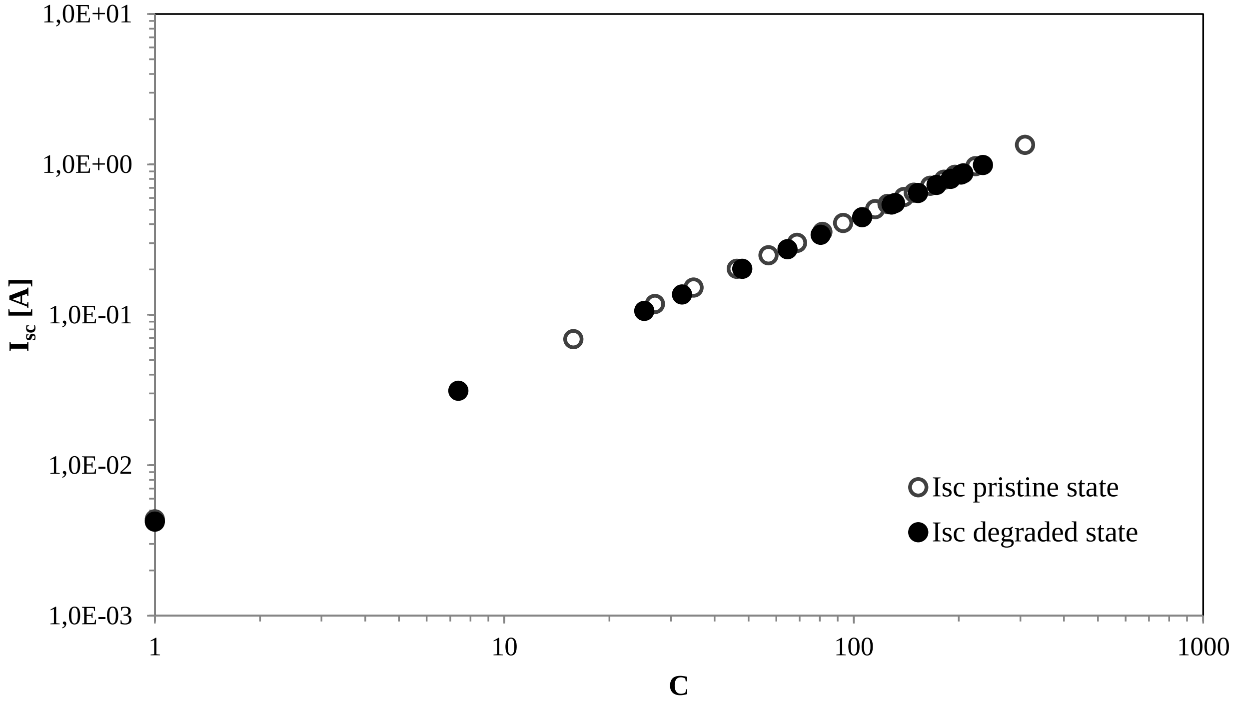

1,0E+01
1,0E+00
1,0E-01
1,0E-02
1,0E-03
I_{sc} [A]
1
10
100
1000
C
Isc pristine state
Isc degraded state

b)

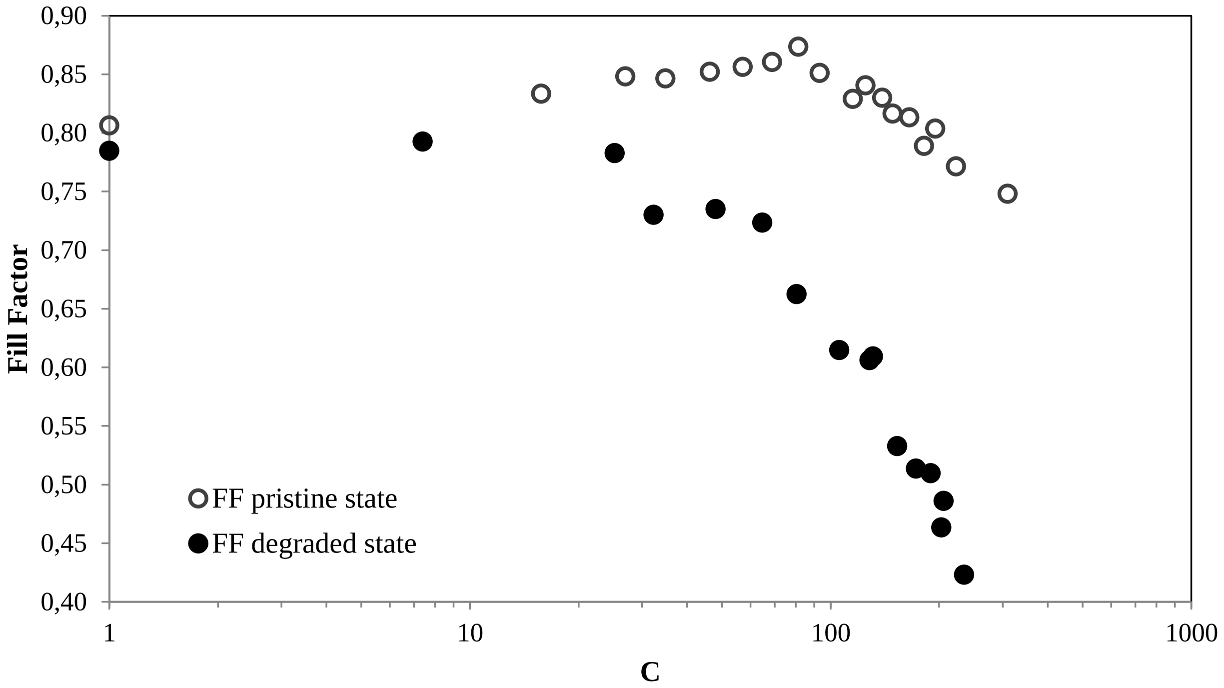

c)

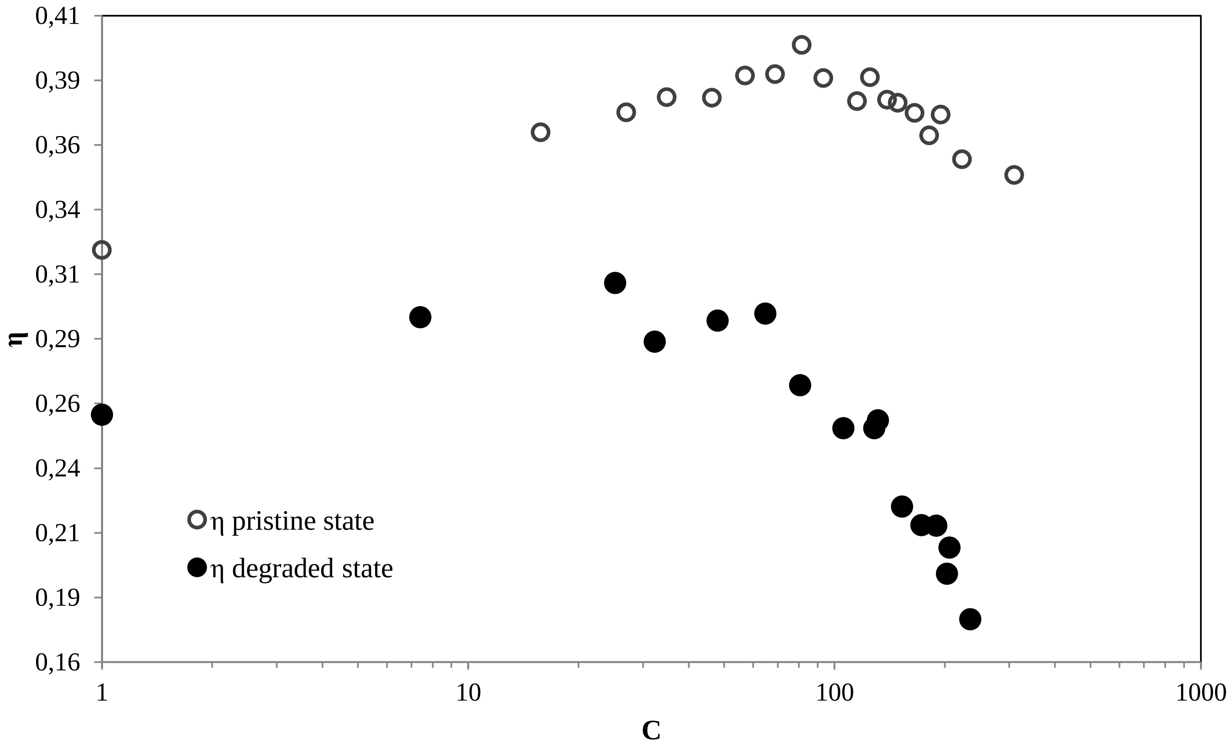

d)

Figure 6 Comparison of the solar cell parameters for the pristine and for the degraded TJ cell as function of C: (a) open-circuit voltage (VOC); (b) short-circuit current (ISC); (c) fill factor (FF); (d) efficiency (η).

Figure(s)

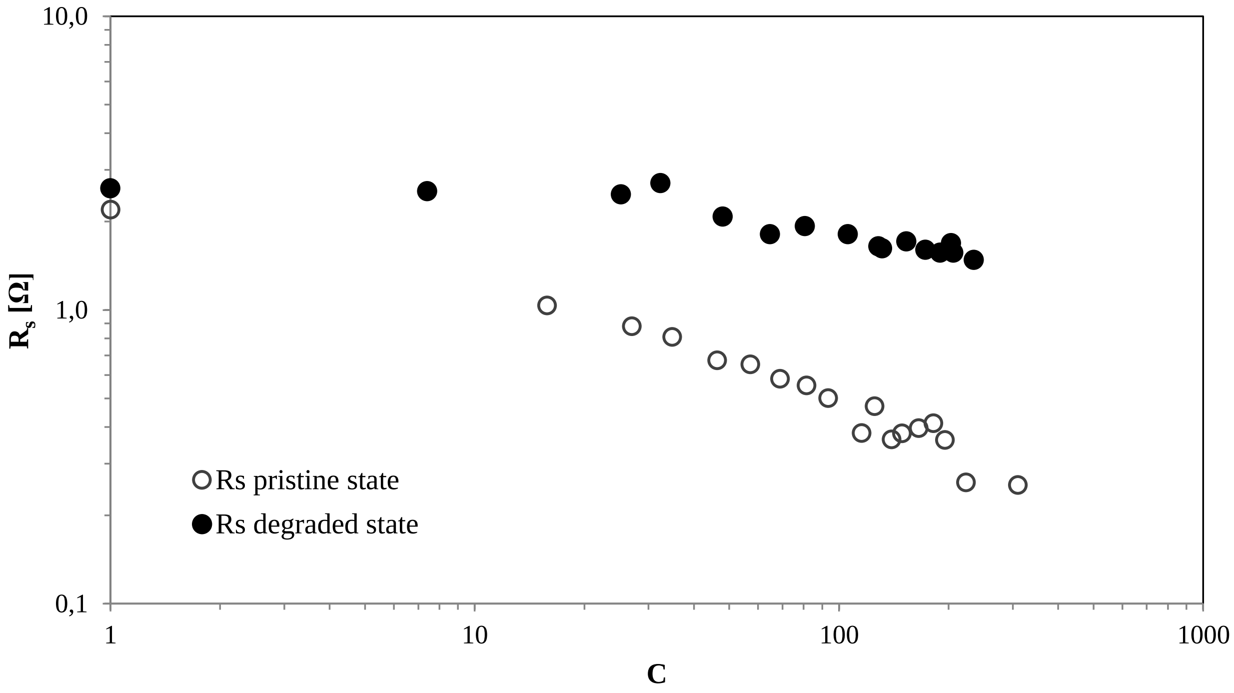

a)

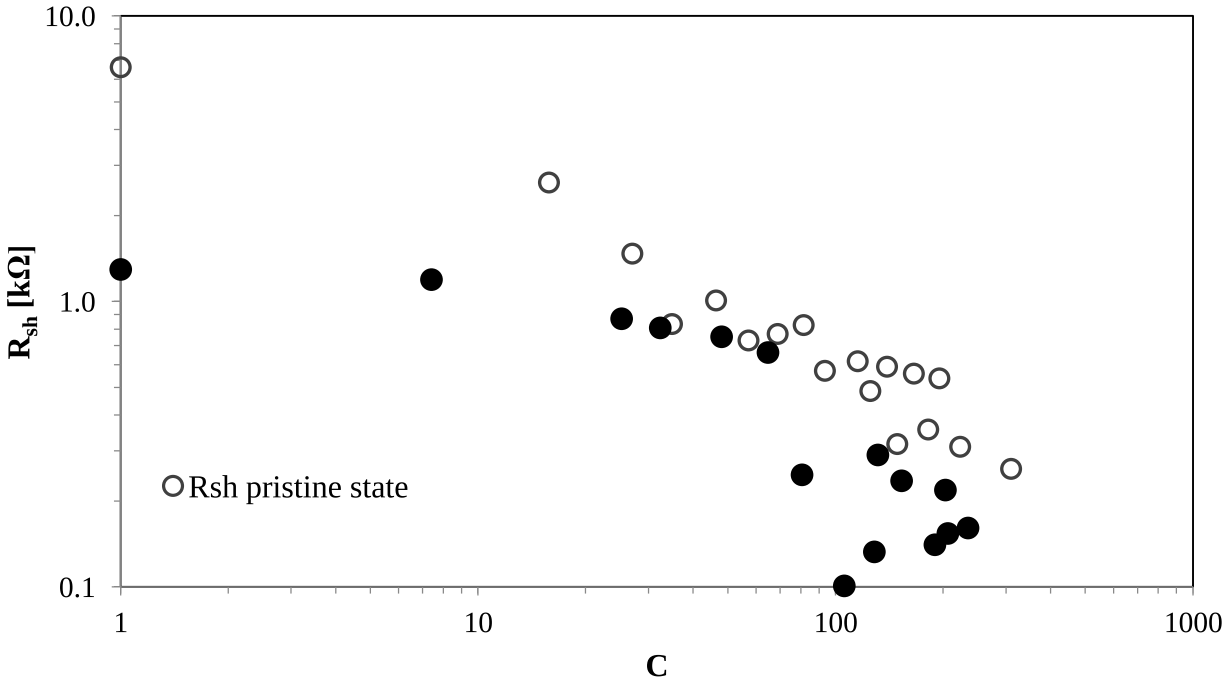

b)

Figure 7 Comparison of the series resistance R_S and of the shunt resistance R_{sh} as function of C for the TJ solar cell in the pristine and in the degraded states

Figure(s)

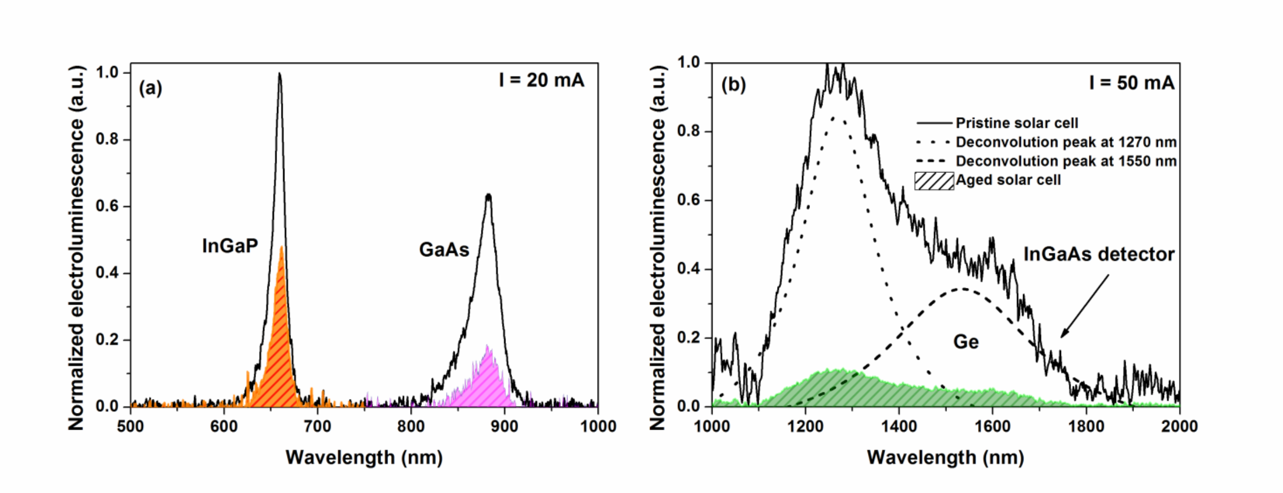

Figure 8 Comparison between the normalized electroluminescence spectra measured for a InGaP/GaAs/Ge triple-junction solar cell biased at different injection currents: (a) I = 20 mA and (b) I = 50 mA in the pristine (dotted line) and (b) in the aged state (solid line).

Figure(s)

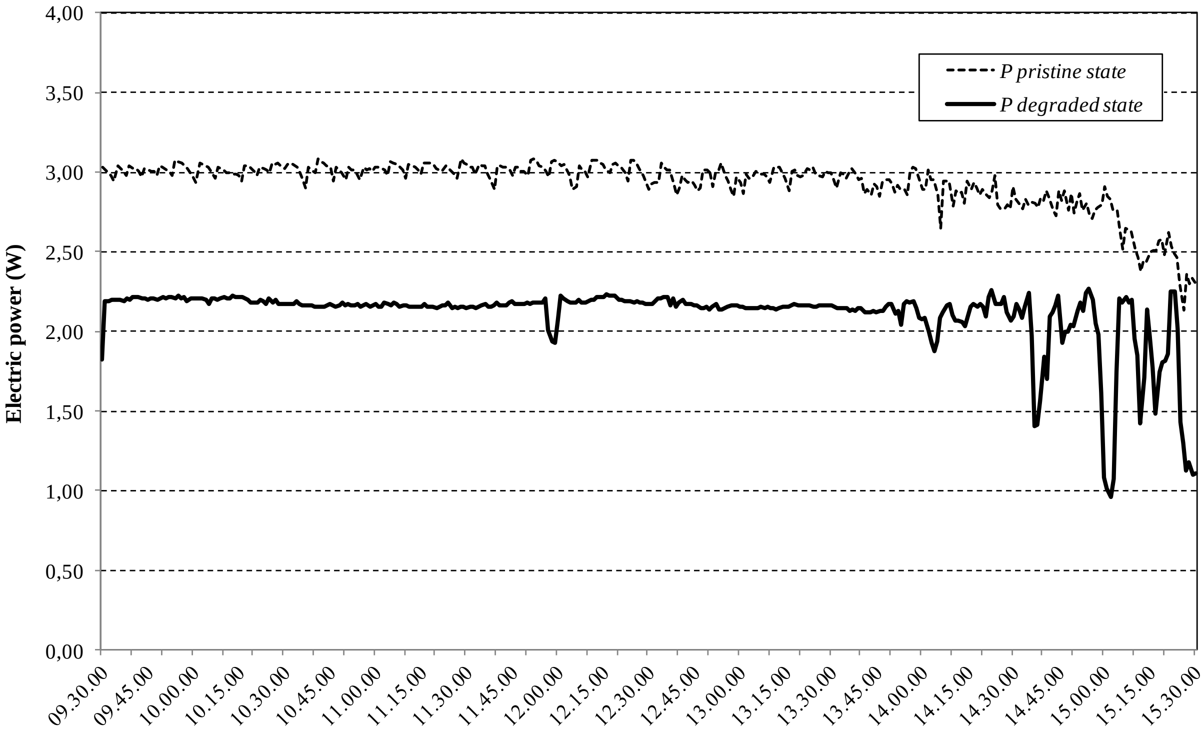

Figure 9 Comparison between the measured electric powers for the TJ solar cell in the pristine and degraded states

Figure(s)

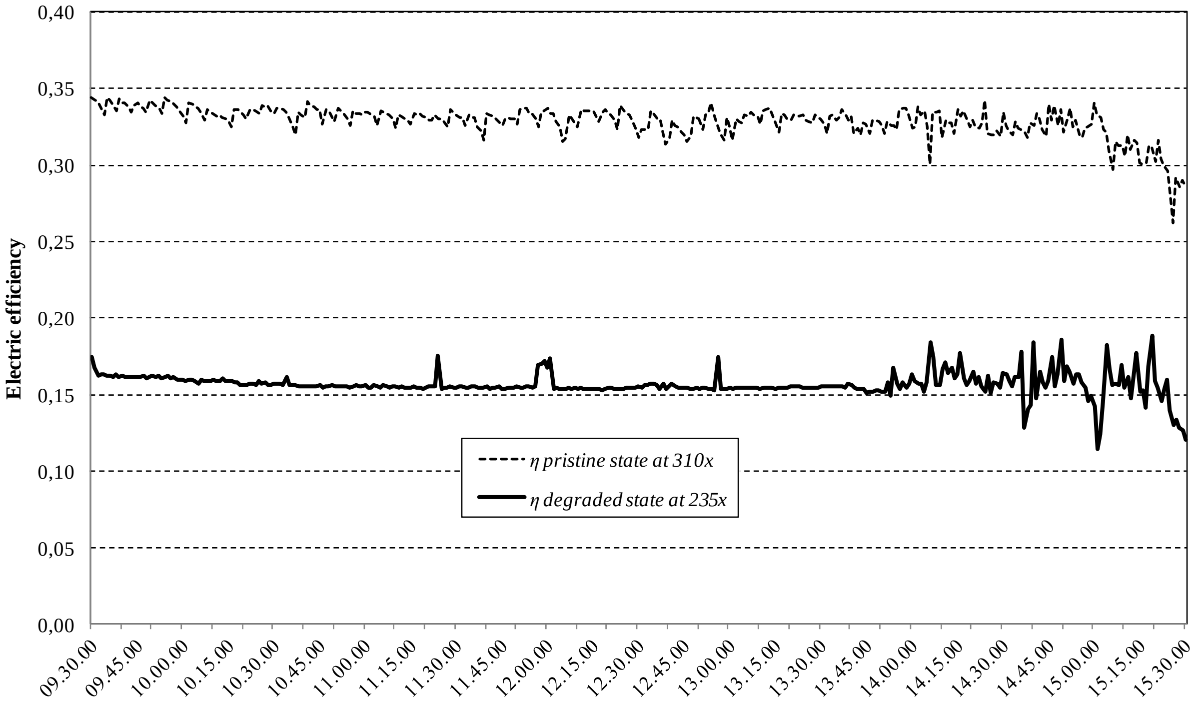

Figure 10 Comparison between the CPV system electric efficiency values with the TJ solar cell in the pristine and degraded states

Figure(s)

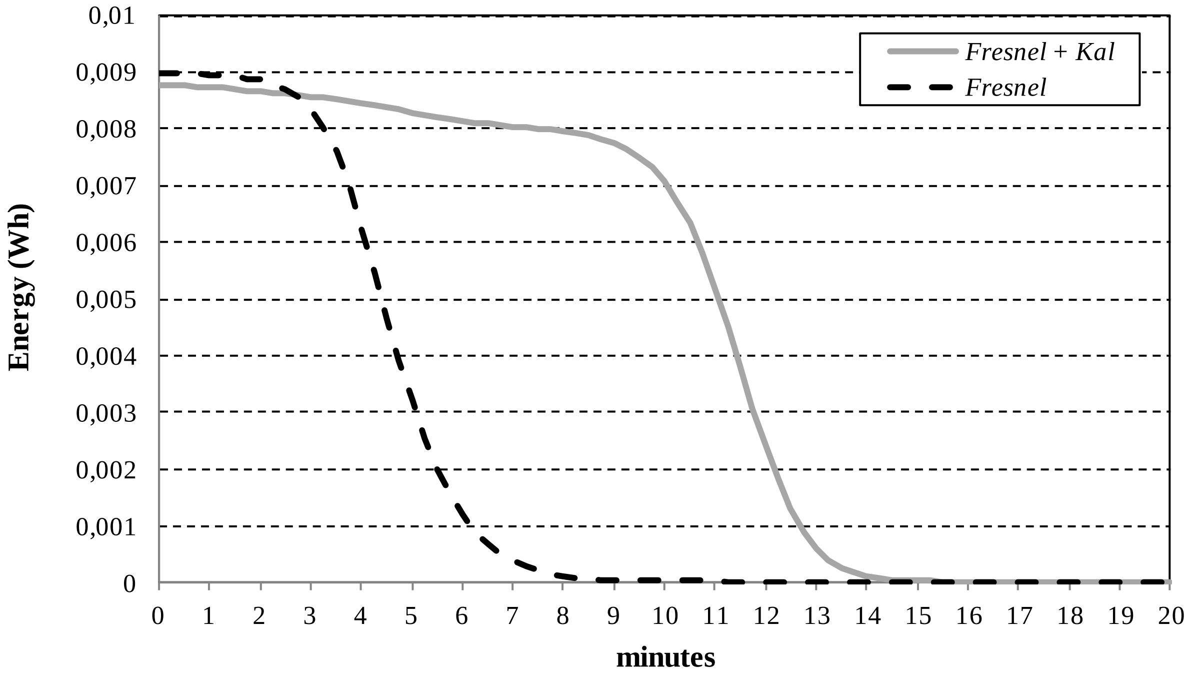

a)

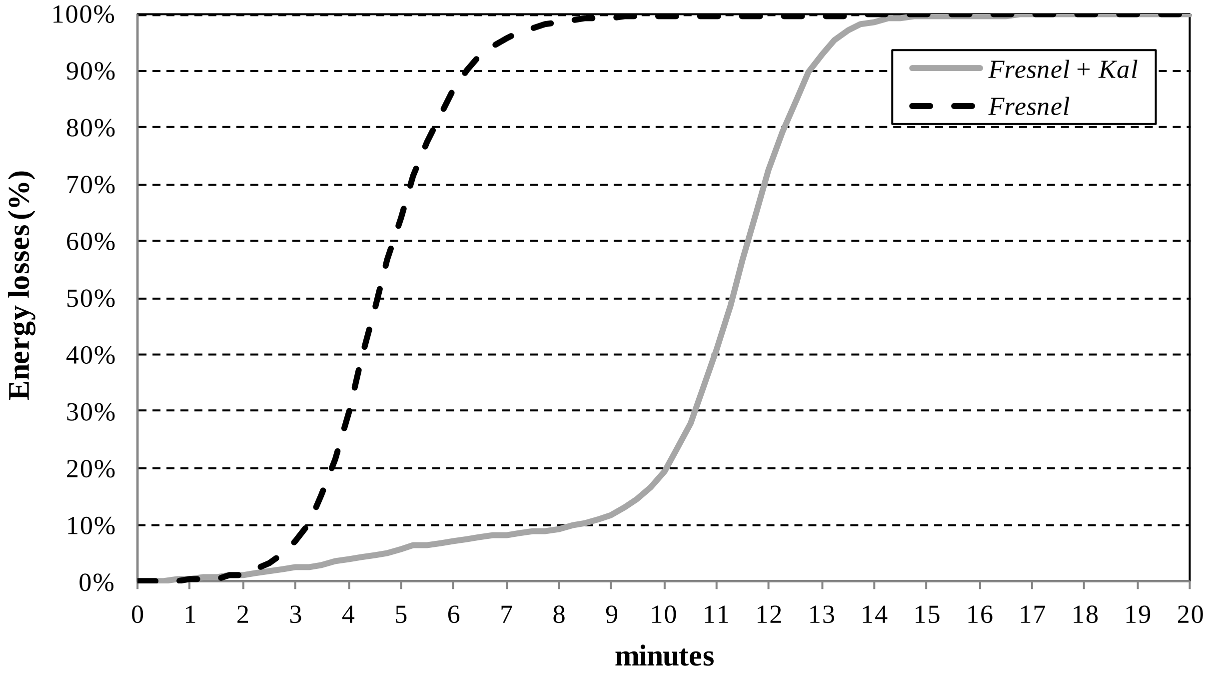

b)

Figure 11 Tracking system problems: (a) energy losses in different configurations; (b) time for a complete interruption.